Journal of Physics: Conference Series **463** (2013) 012055 doi:10.1088/1742-6596/463/1/012055

Development of Soft X-ray Contact-type Microscope and Application to Micro-spectroscopy in Water-window

T. Ejima, Y. Neichi, F. Ishida, and M. Yanagihara

IMRAM, Tohoku University: 2-1-1, Katahira, Aoba-ku, Sendai, 980-8577 JAPAN

ejima@tagen.tohoku.ac.jp

Abstract. A contact-type microscope for the observation of organelles in a culture solution is fabricated with the use of a scintillator plate which shows high quantum efficiency and linearity in Water-window wavelength region. The fabricated microscope was applied to micro –spectroscopy, and an absorption spectrum of polystyrene beads was obtained from SX images taken by the microscope.

1. Introduction

Light in soft X-ray (SX) wavelength region can excite core-level electrons of a material, then chemical bonding states and/or electronic structures of materials can be clarified by core-level spectroscopies using SX light [1]. Especially, the wavelength region between C and O absorption edges (λ=2.3 ~ 4.4 nm) is called Water-window, because the light in this wavelength region is transparent to water comparing with the other wavelength region and organelles will be observed in cultures. If spectra of organelles in bio-cells can be measured at around C, N, and O absorption edges, chemical bonding states of the organelles will be clarified.

When organelles in a bio-cell are observed by use of a SX microscope, the organelles look different from the same organelles observed by a visible (VI) microscope. This is because the contrasts of the organelles in a SX image are different from the ones in a VI image. Then the identification of each organelle in SX images is difficult by itself. In VI wavelength region, several microscopic techniques were developed to observe the organelles [2]. If these techniques are simultaneously used with the SX observation, the organelles will be exactly identified. Therefore, we think that comparison of a SX image with VI images at the same position is necessary to identify organelles in a bio-cell.

As an easy microscopic method to compare a SX image with a VI one, a contact-type microscope was fabricated on a basis of the two-dimensional detector, SXV-IC, which we have developed [3]. In the developed microscope, a transparent SX image is converted to a VI one by a scintillator plate. Moreover the scintillator plate is transparent in VI wavelength region, and then transparent VI images can be observed by the change of the incident wavelength from SX light to VI light. Flexibility of incident wavelength enables us to identify organelles. Application of the microscope to spectroscopic measurements will be presented in this paper.

2. Evaluation of SCOM in Water-window

Optical layout of the fabricated microscope, Soft x-ray COntact Microscope (SCOM), is represented in Figure 1. SX light irradiates a measurement sample through a SiN membrane. The shadow of the incident SX light is converted to a VI image by a scintillator plate placed at the back of

the sample. The converted VI image is magnified by a VI optics through the transparent scintillator plate.

2.1. Sample-cell for bio-cells in culture solution

In the fabricated microscope, a SX shadow of a sample is converted to a VI image by a scintillator plate. Therefore it is desirable that the sample is firmly attached on the scintillator plate, even if the sample is bio-cells in a culture solution. For this purpose, we have fabricated a sample cell for observation of bio-cells in a culture solution.

As represented in Figure 1, a fabricated sample-cell was designed as follows. A sample being measured is pressed on a scintillator plate by a SiN membrane. The SiN membrane adhered on a stainless-steel plate was 100 nm thick and 0.25 × 0.25 mm^2 in window size. The scintillator plate was adhered on another stainless-steel plate and was 0.2 mm thick and 4.5 mm in diameter. Both the stainless-steel plates were set to a base with O-rings not to leak the solution from the cell.

To check a leak-rate from the sample-cell, the sample-cell with and without water was placed into a vacuum chamber. Then partial pressure of H_2O was measured. The measurement was made by quadrupole mass filter (CANNON-ANELVA, M-101QA-TDM) before and after the placement of the sample-cell into the vacuum chamber. Base pressure was 2.3×10^{-6} Pa before the placement, and that was 4.4×10^{-6} Pa after the placement. Difference between the values was caused by the pumping time before and after the placement. After the measurements, the water remained in the sample-cell.

The change of the partial pressure rate is plotted in Figure 2. Zero point of the horizontal axis in Figure 2 is 30 minutes after the placement into the vacuum chamber to avoid an initial fluctuation of the pressure caused by the introduction of the sample-cell. As it can be seen from the figure, the change of the pressure rate was nearly equal to each other.

2.2. Quantum efficiency of the scintillator

Scintillator material is a key component in the system because of the quality of SX images depending on specifications of the scintillator plate. The specification that relates to SCOM is quantum efficiency $q_{scin}(\lambda_{SX})$ for a wavelength λ_{SX} in SX region. Using quantum efficiency $q_{scin}(\lambda_{SX})$ of the scintillator plate, numerical aperture of VI objective lens *NA*, transmittance of VI microscope $T_{VIM}(\lambda_{scin})$ at the luminescence wavelength λ_{scin} of the scintillator material, and quantum efficiency $q_{CCD}(\lambda_{scin})$ of the CCD image sensor, total quantum efficiency $Q(\lambda_{SX})$ of SCOM is represented as

$$Q(\lambda_{SX}) \propto q_{scin}(\lambda_{SX})\, T_{VIM}(\lambda_{scin})\, q_{CCD}(\lambda_{scin}) \left(1-\sqrt{1-NA^2}\right). \quad (1)$$

Except for the quantum efficiency $q_{scin}(\lambda_{SX})$ of the scintillator, all parameters are known: transmittance of the VI microscope is more than 0.8 and dispersion of the transmittance is flat [4], quantum efficiency of the CCD image sensor is 0.63 at the luminescence wavelength λ_{scin} [5]. Therefore, total quantum efficiency $Q(\lambda_{SX})$ can be obtained from measurement results.

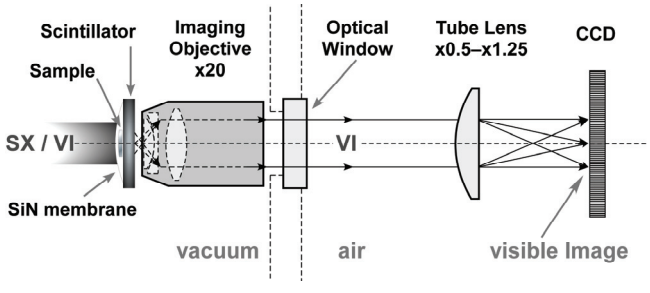

Figure 1. Schematic representation of SCOM.

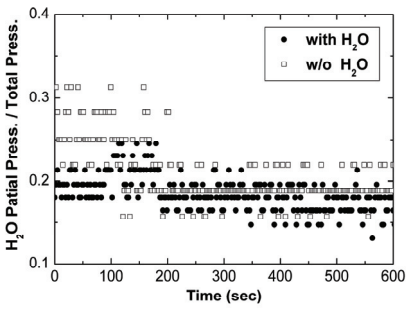

Figure 2. Change of partial pressure H_2O.

We chose Ce:LYSO (Oxide Co., Japan) as a material of the scintillator plate, because its quantum efficiency is high in SX region and it has no deliquescence [3]. Both sides of the scintillator plate were optical-polished and its quantum efficiency was measured with the use of SCOM. The values of relative quantum efficiency were determined by Equation (1). All measurements were carried out at beamline BL11D in Photon Factory, KEK, Japan under the following conditions: wavelength resolution was 500, wavelength of incident light, 2 ~ 5 nm, and exposure time depending on the photon intensity, 5 ~ 30 sec [6].

Measured spectrum of relative quantum efficiency is plotted in Figure 3. The efficiency decreases slowly as the increase of the wavelength, and show a local minimum value at 2.3 nm. The efficiency decreases again from 2.4 nm and shows the minimum value at around 4.4 nm. The efficiency increases from 4.4 to 5 nm. The small dip structure at 2.3 nm is O-K absorption edge, which is originated from the component atoms in the mother material of the scintillator. The minimum value at 4.4 nm will be caused by C-K absorption edge, and its origin will be C atoms remained on the surface of the scintillator plate, because the plate was rinsed out by ethanol and acetone solutions.

2.3. Spatial resolution

Spatial resolution was measured by an edge response of a polystyrene bead in water. The measurement was made by the same setup of the quantum efficiency measurement under the following conditions: measurement wavelength region was 2.1 ~ 4.4 nm, wavelength resolution, 500, and exposure time depending on the photon intensity, 240 ~ 300 sec. An image of polystyrene beads in water taken at wavelength 2.30 nm is presented in Figure. 4 (a). Black points were the polystyrene beads in the figure, and the other area was water. The black points showed no movement during the exposure, therefore the beads were considered to be fixed on the scintillator plate.

Intensity profile of the beads was made as follows: the several points were selected and intensity profiles were averaged. The intensity profile was fitted by Gaussian curve to estimate the HWHM value as the spatial resolution. Obtained profile is designated as black circles in Figure 4 (b), the fitting result is as a solid curve. The HWHM value was 0.72 μm, it is comparable with the ideal value, 0.69 μm, under the conditions that numerical aperture of objective lens was 0.4 and observation wavelength, 450 nm [7].

3. Application to micro-spectroscopy

When the fabricated microscope was applied to micro-spectroscopy measurement, polystyrene beads in water were chosen as a standard sample. Observation conditions were the same as the evaluation of spatial resolution, and one of the SX images has been presented in Figure. 4(a). Spectrum of a region of interest (ROI) was obtained as follows: **1.** SX images of the irradiation light were observed by SCOM changing the incident wavelength. **2.** SX images of the sample were observed as well as the irradiation light. **3.** Sample image was normalized by the exposure time and then normalized by the irradiation light image at the same incident wavelength. Obtained images are transmittance ones. **4.** A ROI to obtain a spectrum is determined referring to the same ROI of VI

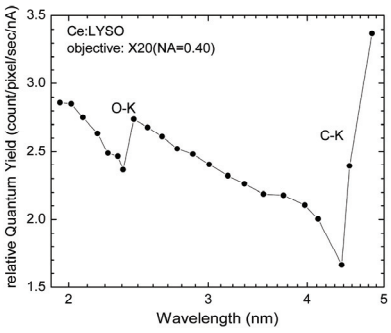

Figure 3. Relative quantum efficiency of Ce:LYSO.

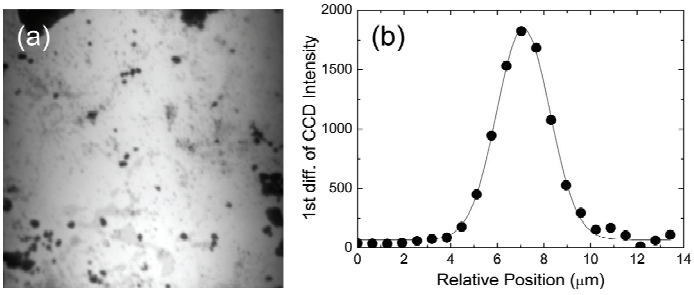

Figure 4. a) Polystyrene beads image at a wavelength 2.30 nm. b) Edge response of the beads in water. HWHM was 0.72 μm.

images, and intensities of pixels in the ROI are averaged. The intensity-change according to the wavelength was the transmittance of the ROI. **5.** Finally, absorptance of the ROI is obtained on the assumption that there is no interference in the sample.

Beads and water areas were selected as ROIs, and the spectra of both ROI were obtained. Thickness of the sample was less than 1μm, which was estimated from the absorptance of the water. Therefore optical density spectrum of the beads can be calculated. The obtained spectra are plotted in Figure. 5. Peak structures observed at 2.3 nm, 3.1 nm, and 4.3 nm are O-K, N-K, and C-K absorption edges, respectively.

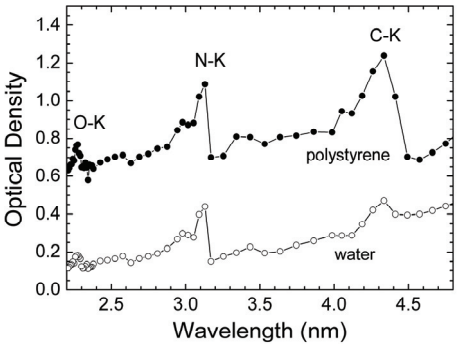

Figure 5. Optical density spectra of both polystyrene beads and water.

The N-K absorption edge peaks were observed in both the beads area and the water one, therefore the peaks are originated from the SiN membrane. As same as the N-K edge peaks, the O-K absorption peaks of both ROIs showed the same shape and almost the same intensity. Therefore, the peaks will be originated from the water in the cell. The C-K absorption edge peaks show the different shape between the beads and the water. The origin of the peak in the polystyrene beads is understood by two major peaks of π and σ bands in polystyrene [8]. The polystyrene-beads peak is broadened by the wavelength resolution and rough wavelength interval, therefore the shape of the peak looks a long tail toward the short wavelength side. The peak intensity in water is small and its width is narrow comparing with the peak of the polystyrene beads. The different shape of the peak suggests that the origin of the peak is the contamination of the SiN window.

4. Summary

A soft X-ray contact-type microscope, SCOM, for taking SX images and obtaining spectra from the images was fabricated and evaluated. The evaluation results showed that transmittance spectrum of polystyrene beads can be obtained after taking SX images. Then spatial resolution of SCOM was measured by edge response method, and its value coincides with the ideal diffraction-limit one. These results suggest that a small organelles identified by visible-light observation can be measured using SX wavelength region by SCOM. It will be a powerful analytical tool to determine not only chemical changes in a biological sample but also electronic structures of nanostructures in a solution.

References

[1] F de Groot & A Kotani, Core level spectroscopy of solids, (CRC Press (Taylor & Francis G.), 2008, Boca Raton) p. 23
[2] for example, B Alberts, *et al.*, *Molecular biology of the cell*, (Garland Science, Taylor & Francis Group, New York, 2010) Chap. 9.
[3] T Ejima, *et al.*, AIP CP **1234**, (2010) 811.
[4] Datasheet of Objective lens, UV Series for ultraviolet rays, Union Optical Co. Ltd.
[5] Datasheet of CCD sensor, CCD47-10, e2v technologies Ltd.
[6] Photon Factory activity Report 1997 #15 (1997) A101., http://pfwww.kek.jp/users_info/station_spec/bl11/bl11d.html
[7] for example, D Attwood, *Soft X-rays and extreme ultraviolet radiation*, (Cambridge University Press, Cambridge, 2000) Chap. 9.
[8] D A Fischer, G E Mitchell, A T Yeh, J L Gland, Appl. Surf. Sci., **133** (1998) 58.